Novel magnetic phases in $La_{0.7}Sr_{0.3}Co_{1-y}Fe_yO_3$ $(0.0 \leqslant y \leqslant 1.0)$: a neutron diffraction study

1998 J. Phys.: Condens. Matter 10 4045

(http://iopscience.iop.org/0953-8984/10/18/014)

J. Phys.: Condens. Matter **10** (1998) 4045–4055. Printed in the UK PII: S0953-8984(98)81286-1

Novel magnetic phases in $La_{0.7}Sr_{0.3}Co_{1-y}Fe_yO_3$ ($0.0 \leqslant y \leqslant 1.0$): a neutron diffraction study

V G Sathe†, S K Paranjpe‡, V Siruguri§ and A V Pimpale†

† Inter University Consortium for DAE Facilities, University Campus, Khandwa Road, Indore 452 001, India

‡ Solid State Physics Division, BARC, Trombay, Mumbai 400 085, India

§ Inter University Consortium for DAE Facilities, BARC, Trombay, Mumbai 400 085, India

Received 24 January 1997, in final form 5 January 1998

Abstract. Magnetic and structural studies in the series $La_{0.7}Sr_{0.3}Co_{1-y}Fe_yO_3$ ($0.0 \leqslant y \leqslant 1.0$) have been carried out by powder neutron diffraction for seven compositions corresponding to $y = 0.0$, 0.1, 0.2, 0.3, 0.5, 0.7, 1.0. At one extreme of this series $La_{0.7}Sr_{0.3}CoO_3$ is a metallic ferromagnet with rhombohedral structure while the other end member $La_{0.7}Sr_{0.3}FeO_3$ is an antiferromagnetic insulator with orthorhombic structure. The transition from rhombohedral to orthorhombic crystal structure is observed with $y \geqslant 0.5$. Ferromagnetic phase is observed for $y \leqslant 0.2$ and antiferromagnetic order is observed for $y > 0.5$. Coexistence of ferro- and antiferromagnetic order is observed for $y = 0.5$. This is supported by ac susceptibility measurements.

1. Introduction

Perovskite compounds $La_{1-x}(Sr, Ba, Ca)_xBO_3$ have been extensively studied for over four decades due to their unique magnetic and transport properties and possible applications [1, 2]. In these compounds the rare earth element plays a steric role to stabilize the structure, and the electronic ground state of transition metal (TM) 'B' decides the magnetic and transport properties. The similarity of the structure to high-T_c superconductors and recent observation of giant magneto-resistance in hole doped $LaMnO_3$ have sparked renewed interest in these compounds [3–5]. Recently, a structural transition from orthorhombic to rhombohedral has been shown to occur with the application of magnetic field in $La_{1-x}Sr_xMnO_3$ for $x = 0.17$ [6]. Replacement of La by Sr not only changes the valence of the TM but also introduces a pressure effect in the lattice, which changes the tolerance factor of perovskite oxide [7]. This implies that the TM–O–TM interatomic distance and bond angle play decisive roles in determining the structural and magnetic properties in these oxides. Hwang *et al* [8] have reported that in these series of compounds resistivity shows an anomalous change at the Curie temperature T_C.

The parent compound $LaCoO_3$ does not show long-range magnetic order down to 4.2 K [9]. This is explained by the fact that Co^{3+} ions are in low-spin state at low temperatures giving the atomic spin $S = 0$. It shows a low-spin–high-spin transition as a function of temperature at 90 K accompanied by an anomalous change in thermal expansion [10]. $La_{1-x}Sr_xCoO_3$ crystallizes in rhombohedral structure and shows a para- to ferromagnetic transition for $x \geqslant 0.2$ [11, 12]. The metal–insulator (M–I) transition is observed at the

0953-8984/98/184045+11$19.50

same composition [11]. These compounds show itinerant ferromagnetic behaviour and the double-exchange mechanism proposed by Zener [13] and further extended by de Gennes [14] explains it qualitatively. Itoh *et al* [15] have given a phase diagram of these compounds showing an insulating spin glass phase for $x < 0.18$ and cluster glass phase for $x \geqslant 0.18$. Our neutron diffraction studies on these compounds show a ferromagnetic order for samples with $0.2 \leqslant x \leqslant 0.5$ [12].

$La_{1-x}Sr_xFeO_3$ crystallizes in the orthorhombic crystal structure. Antiferromagnetic insulating behaviour is reported for $x \leqslant 0.4$ [16]. This shows that the negative exchange coupling is strong in these compounds unlike the corresponding cobalt compounds which have positive exchange for $x \geqslant 0.2$. Recently, charge ordering of Fe^{3+} and Fe^{4+} ions has been reported in $La_{0.7}Sr_{0.3}FeO_3$ [17]. With ferro- and antiferromagnetic ordering exhibited by the Co and Fe based systems, respectively, the mixed series of compounds like $La_{0.7}Sr_{0.3}Co_{1-y}Fe_yO_3$ gives an opportunity to study structural, magnetic and transport properties with competing ferro- and antiferromagnetic interactions.

We have prepared the series $La_{0.7}Sr_{0.3}Co_{1-y}Fe_yO_3$ in the range $0.0 \leqslant y \leqslant 1.0$ and performed neutron diffraction experiments in the temperature range of 300 K to 10 K to study the structural and magnetic behaviour. We report in this paper antiferromagnetic order for $La_{0.7}Sr_{0.3}FeO_3$ ($y = 1.0$), ferromagnetic order for $y = 0.0$, 0.1, 0.2 and coexistence of ferro- and antiferromagnetic order in the $La_{0.7}Sr_{0.3}Co_{1-y}Fe_yO_3$ series for the $y = 0.5$ composition. The coexistence of both the magnetic orders in the $y = 0.5$ composition is also supported by ac susceptibility results.

2. Experimental details

The samples were prepared by the solid state reaction method using spectroscopically (99.9%) pure materials as starting constituents. The solid solution obtained by heating the nitrates of all constituent materials was ground and sintered at 930 °C for 24 hours. The process of grinding and heating was repeated five times. Final sintering was performed in oxygen atmosphere for 24 hours. Powder x-ray diffraction patterns showed the formation of a single phase compound and no impurity line was seen.

Neutron diffraction measurements were carried out on the PSD-based powder diffractometer at Dhruva reactor, BARC, using a wavelength of 1.094 Å [18]. Samples were well ground and packed in cylindrical vanadium containers for room-temperature measurements. For low-temperature experiments the samples were packed in an aluminium can attached to the cold finger of a closed cycle refrigerator (CCR).

The room-temperature patterns for $y = 0.0$, 0.1, 0.2, 0.3, 0.5, 0.7, 1.0 were recorded in the angular range of 10° to 80°. In order to observe the magnetic ordering, diffraction profiles were recorded at 10 K for $y = 0.1$, 0.2 and 1.0 samples, and at 10, 50, 100, 150, 200 K for the $y = 0.5$ sample.

The real part of ac susceptibility (χ) for the $y = 0.5$ composition was measured using a mutual inductance bridge at 13 Oe applied field and 133 Hz frequency from 300 K down to 78 K.

3. Experimental results

3.1. Room-temperature measurements

$La_{0.7}Sr_{0.3}CoO_3$ crystallizes in the rhombohedral structure ($R\bar{3}C$) with two chemical formula units per cell while $La_{0.7}Sr_{0.3}FeO_3$ has an orthorhombic structure ($Pbnm$) with four chemical

Table 1. Various structural parameters obtained from the Rietveld refinement along with the factors indicating goodness of the fit.

Parameter	$y = 0.1$	$y = 0.2$	$y = 0.3$	$y = 0.5$	$y = 0.7$	$y = 1.0$
Structure	Rho.	Rho.	Rho.	Orth.	Orth.	Orth.
Cell parameter (Å)						
a	5.406(4)	5.417(9)	5.422(6)	5.396(5)	5.475(3)	5.502(8)
b	5.406(4)	5.417(9)	5.422(6)	5.458(6)	5.536(5)	5.544(4)
c	5.406(4)	5.417(9)	5.422(6)	7.719(7)	7.848(8)	7.846(5)
$\alpha = \beta = \gamma$	60.392(7)	60.411(6)	60.330(4)	90.00	90.00	90.00
O$x1$	0.212(2)	0.210(1)	0.211(2)	−0.014(1)	−0.001(1)	0.069(2)
O$y1$	0.287(1)	0.289(1)	0.288(1)	0.472(1)	0.469(2)	0.455(3)
O$z1$	0.75	0.75	0.75	0.25	0.25	0.25
O$x2$				0.234(2)	0.238(2)	0.248(1)
O$y2$				0.265(2)	0.261(2)	0.251(1)
O$z2$				−0.03(1)	−0.037(1)	−0.023(1)
Cell volume V						
per formula unit (Å^3)	56.36(5)	56.73(6)	56.80(5)	56.83(5)	59.49(8)	59.84(6)
R_p	7.39	7.69	7.63	7.56	7.80	7.85
R_{exp}	7.45	7.7	7.55	7.86	7.92	7.65
R_{wp}	9.34	9.80	9.68	9.53	9.90	10.56

$R_p = 100 \sum |y_{oi} - y_{ci}| / \sum |y_{oi}|$, the pattern R-factor.
$R_{wp} = 100\{\sum w_i (y_{oi} - y_{ci})^2 / \sum w_i (y_{oi})^2\}^{1/2}$, the weighted pattern R-factor.
$R_{exp} = 100\{(N - P + C)^2 / \sum w_i (y_{oi})^2\}^{1/2}$, the expected pattern R-factor where y_{oi} is the observed (gross) intensity at the ith step, y_{ci} is the calculated intensity at the ith step, w_i is the weighting factor, N is the total number of data points 'observations', P is the number of parameters adjusted and C is the number of constraints applied.

formula units per cell. The series $La_{0.7}Sr_{0.3}Co_{1-y}Fe_yO_3$ is thus expected to show a structural transition from rhombohedral to orthorhombic with increasing y. Structural analyses were carried out for room-temperature (297 K) data using the modified version of the profile refinement program by Young *et al* [19]. The parameters varied during refinement were atomic positions, occupancies and temperature factors in addition to the instrumental parameters such as zero angle, half-width parameters and scale factor. The observed and the fitted patterns for $y = 0.3$ and $y = 0.5$ are shown in figure 1. The patterns for $y \leqslant 0.3$ fitted well with the rhombohedral $R\bar{3}C$ space group. Attempts were also made to fit using the orthorhombic space group $Pbnm$. However, the agreement between observed and calculated patterns was poor. A two-phase model, using both rhombohedral space group $R\bar{3}C$ and orthorhombic space group $Pbnm$, was also attempted for $y = 0.3$. The phase analysis of this model showed 97% of rhombohedral structure against 3% of orthorhombic structure. The corresponding agreement factor R_p was 7.9 against 7.6 for the single-phase model. Thus, up to $y = 0.3$ the compounds have rhombohedral crystal structure. A similar analysis is done for the $y = 0.5$ sample. In this case phase analysis resulted in 95% of orthorhombic phase against 5% of rhombohedral phase. The corresponding R_p obtained was 7.9 against 7.5 for single-phase $Pbnm$ space group. The samples with $y = 0.7$ and 1.0 were fitted with a single-phase model with the orthorhombic space group. To check the oxygen stoichiometry oxygen occupancies were refined, as the magnetic and transport properties of perovskite oxides are reported to be sensitive to the oxygen stoichiometry. The oxygen occupancy has not shown significant variation from its full value during refinement, thus establishing the stoichiometry of the samples. Refined structural parameters obtained are summarized in table 1. The bond lengths and bond angles are given in table 2.

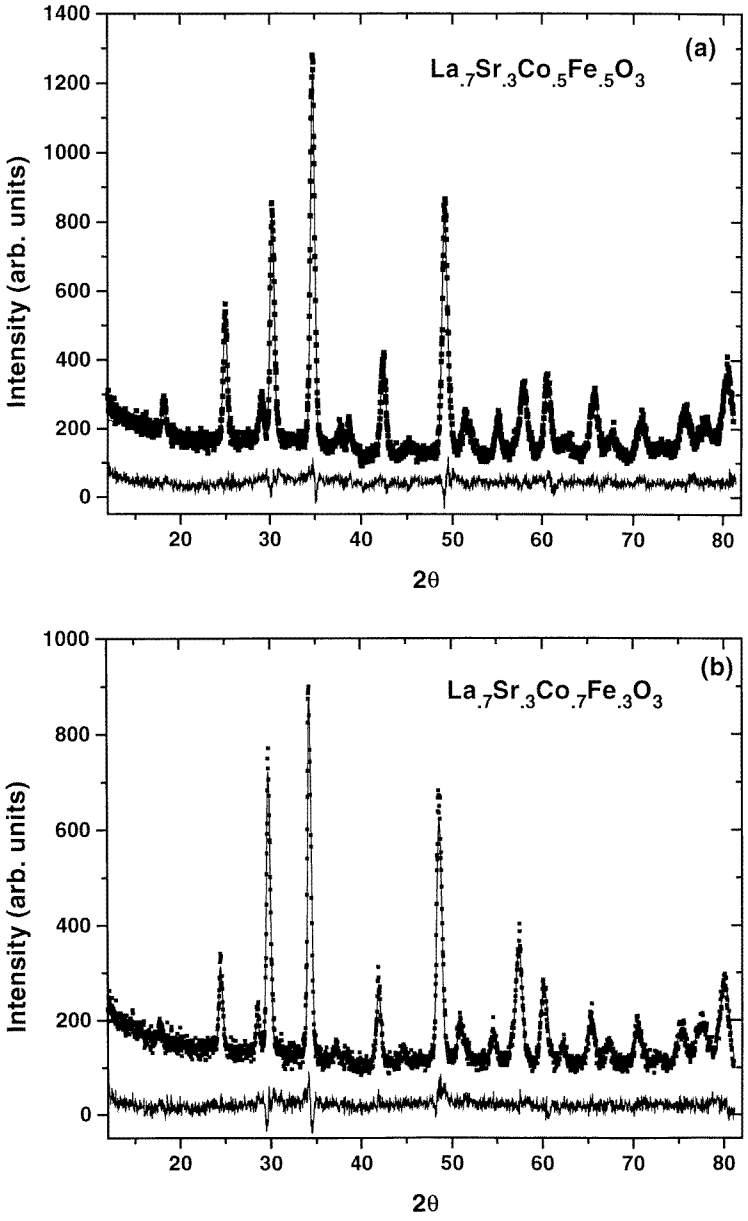

Figure 1. The observed and fitted patterns along with the difference curve at the bottom for (a) $y = 0.5$, (b) $y = 0.3$.

Replacement of Co ion by Fe ion induces an increase in unit-cell volume. The increase in unit-cell volume with increase in Fe concentration y is in agreement with the larger ionic radius of the Fe ion as compared to the Co ion. The average TM–O distance increases, while the TM–O–TM bond angle deviates from 180° as the crystal structure changes from rhombohedral to orthorhombic. The deviation of the bond angle from 180° indicates greater distortion in the oxygen octahedra.

Table 2. Various bond-length (Å) and bond-angle (deg) parameters obtained for $La_{0.7}Sr_{0.3}Co_{1-y}Fe_yO_3$.

Parameters	$y = 0.1$	$y = 0.2$	$y = 0.3$	$y = 0.5$	$y = 0.7$	$y = 1.0$
Co–O	1.927(4)	1.933(3)	1.933(2)	1.934(2)	1.969(9)	1.981(2)
La–O	2.715(3)	2.722(2)	2.723(3)	2.793(1)	2.770(2)	2.779(5)
Co–O_I–Co	167.798(4)	167.452(3)	167.676(9)	166.031(2)	162.766(3)	159.349(5)
Co–O_{II}–Co				169.812(7)	170.223(8)	167.360(4)

Table 3. Moment per TM ion in μ_B obtained from integrated intensity at 10 K and 300 K.

	300 K	10 K	
Composition	AFM	AFM	FM
$y = 0.0$[a]	—	—	1.89(11)
$y = 0.1$	—	—	1.2(1)
$y = 0.5$	0.4(2)	1.18(8)	0.6(2)
$y = 0.7$	0.7(2)		
$y = 1.0$	2.1(9)	2.52(11)	
$LaFeO_3$[b]		4.6(3)	

[a] Values as quoted in [12].
[b] Values as quoted in [24].

3.2. Low-temperature data

3.2.1. Co-rich compounds ($y = 0.1, 0.2$). The diffraction profile for $y = 0.1$ shows an increase in the (110) peak at 10 K as compared to the room-temperature profile indicating ferromagnetic order. The magnetic ordering is similar to that for $La_{0.7}Sr_{0.3}CoO_3$ [12]. With the replacement of Co by Fe ion the effective magnetic moment per TM site shows a decrease as compared to pure $La_{0.7}Sr_{0.3}CoO_3$ (table 3). The 10 K data for $y = 0.2$ also show a very weak peak at the (110) position. There is no signature of any antiferromagnetic ordering down to 10 K.

3.2.2. Pure Fe compound ($y = 1.0$). The diffraction profiles for $y = 1.0$ were recorded at 10 K and at room temperature. This sample shows antiferromagnetic order at room temperature. From structure factor calculations it is seen that only peaks with $h+k = 2n+1$ and $l = 2n' + 1$ (with n' positive integers) will have magnetic contributions. At 10 K, the intensities of antiferromagnetic peaks {(011), (101)} and {(121), (103), (211)} show an increase while all other peaks remain unaltered. No sign of ferromagnetic ordering is seen in this sample. Room-temperature and 10 K data were refined using the FULLPROF [20] profile refinement program. Magnetic structure parameters were also included in the refinement. It is difficult to conclusively assign the direction of the site moment due to inability to resolve the (011) and (101) reflections. An attempt is made to fit the peak with two Gaussian peaks which resulted in the ratio of intensities under (011) and (101) peaks being 10/3, suggesting that the moment lies along the [100] direction [21]. Henceforth, in the refinement, we have used [100] as the direction of the moment. The fitted pattern is shown in figure 2. The goodness of fitting factors (for definition see table 1) resulting are as follows: $R_p = 9.1$ (total); $R_{exp} = 8.5$ (total); R-magnetic 10.1.

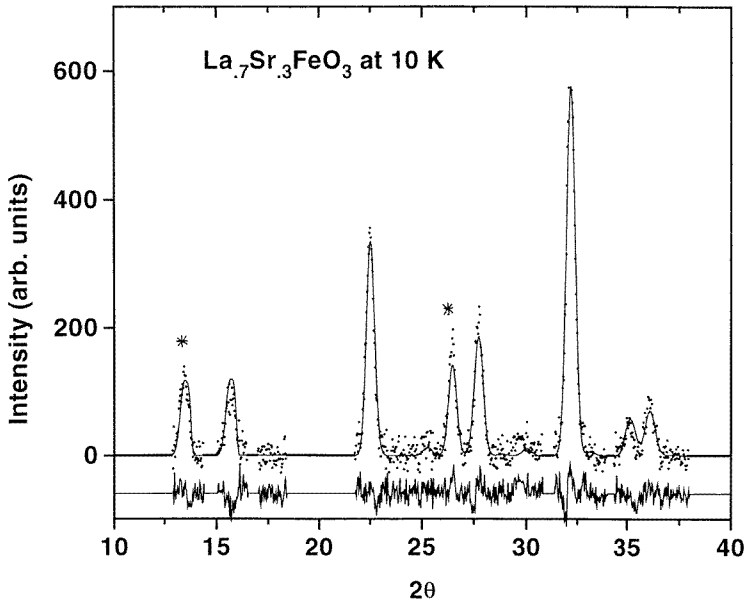

Figure 2. Observed and fitted patterns along with difference curve for $y = 1.0$ at 10 K. The magnetic peaks are marked as $*$.

3.2.3. Intermediate compound ($y = 0.5$). The temperature dependence of the diffraction profile for the $y = 0.5$ sample is shown in figure 3. The solid line is a profile fit. For $y = 0.5$, the pattern at 10 K is refined by taking a three-component model using the FULLPROF refinement program: the first component for nuclear structure; the second for antiferromagnetic structure and the third for ferromagnetic structure. The R-factors resulting are as follows: $R_p = 9.6$ (total); $R_{exp} = 8.9$ (total); R-magnetic $= 10.6$ and R-nuclear $= 9.1$. Three peaks marked as $*$ and ■ in the figure show an increase in relative intensity while the rest of the peaks remain the same as the temperature is lowered. The increase in peaks marked with $*$ is identified with the antiferromagnetic order similar to parent compound $y = 1.0$. The increase in intensity observed in the peak marked as ■ corresponds to the ferromagnetic order. Figure 4 shows the temperature dependence of ferro- and antiferromagnetic peaks. The integrated intensity of peaks corresponding to both ferro- and antiferromagnetic order shows an increase as the temperature is lowered. Figure 5 shows the temperature dependence of antiferromagnetic moment obtained from the neutron data along with the Brillouin function for $S = 5/2$. Figure 6 shows the ac susceptibility versus temperature curve for the $y = 0.5$ composition. Susceptibility shows a decrease as the temperature is lowered from 300 K down to 230 K. Beyond 230 K there is a rise with a broad peak around 100 K, below which it again decreases. The rise in susceptibility below 230 K indicates the onset of ferromagnetic order. It may be remarked that our measurements on pure $La_{0.7}Sr_{0.3}CoO_3$ show a ferromagnetic order setting in around 230 K [12]. A similar transition is reported around this temperature by many workers in $La_{1-x}Sr_xCoO_3$ [15, 22].

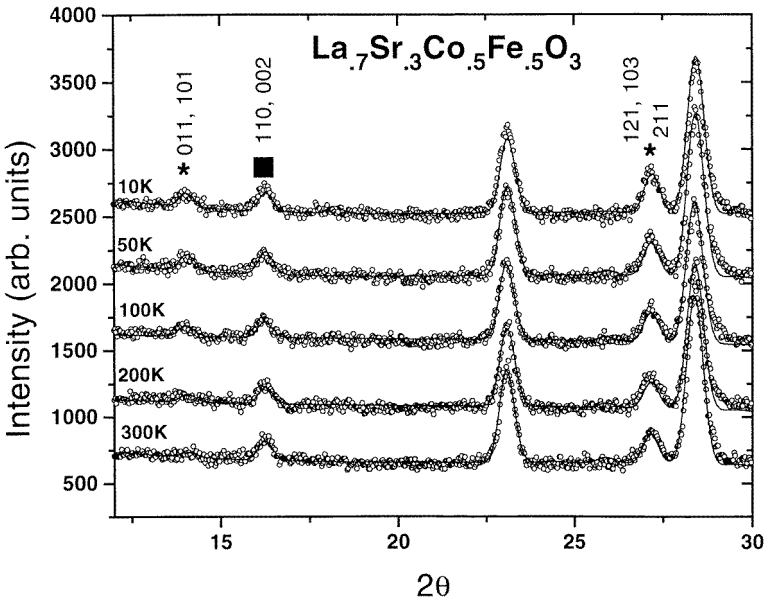

Figure 3. Evolution of magnetic peaks with temperature for $y = 0.5$, $*$ denotes rise in antiferromagnetic order and ■ denotes rise in ferromagnetic order.

4. Discussion

4.1. Co-rich compounds ($y = 0.1, 0.2$)

The Co-rich extreme of this series exhibits ferromagnetic order. The ferromagnetic moment decreases rapidly as the Fe-ion concentration is increased. From $y = 0.1$ the magnetic moment per TM site is found to be 1.2 μ_B at 10 K (table 3). The value of magnetic moment for $y = 0.2$ could not be obtained due to rather poor intensity of the magnetic contribution. Comparing the transition temperature and moment on TM ion in the two end members in this series ($y = 0.0$, $y = 1.0$), we observe that the antiferromagnetic interaction between Fe ions is much stronger than the ferromagnetic interaction between Co ions. Similar behaviour has been reported in $La_{0.5}Ba_{0.5}Co_{1-x}Fe_xO_3$ by Minet *et al* [23] from their magnetization measurements.

4.2. Fe-rich compound ($y = 1.0$)

In pure $LaFeO_3$ it is observed that the Fe^{3+}–O–Fe^{3+} superexchange is responsible for antiferromagnetic order, and the magnetic moment at 5 K on the Fe ion was found to be 4.6 μ_B which is less than the spin only value of the Fe^{3+} ion of 5.0 μ_B per Fe site [24]. Replacement of La by Sr in $La_{0.7}Sr_{0.3}FeO_3$ introduces an additional hole into the system, which transforms Fe^{3+} to Fe^{4+} ions. In this way 30% of the Fe ions are now tetravalent. Introduction of Fe^{4+} ions into the system opens a possibility of double exchange Fe^{3+}–O–Fe^{4+} interaction which is positive in nature. It is reported that, up to 40% Sr concentration, $La_{1-x}Sr_xFeO_3$ remains an antiferromagnetic insulator and magnetic moment

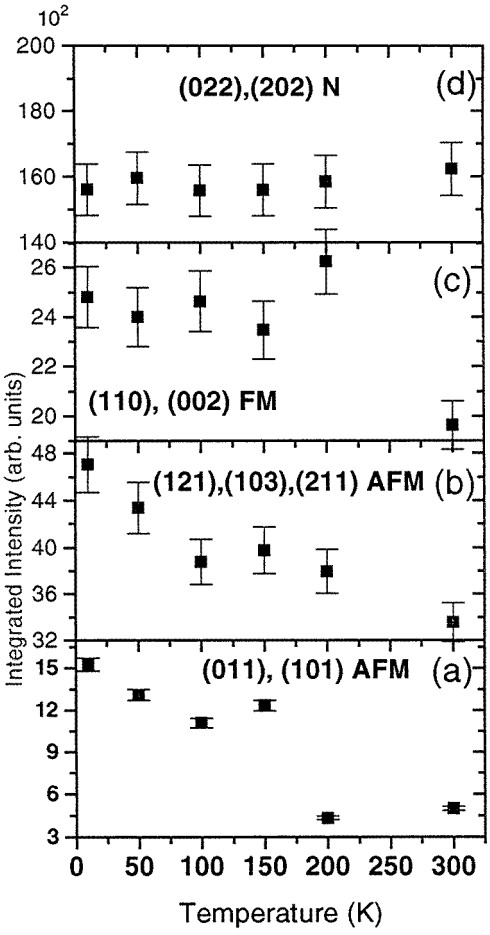

Figure 4. Temperature dependence of integrated intensity of magnetic peaks. (a) and (b) show evolution of antiferromagnetic order, (c) shows ferromagnetic order. Integrated intensity of nuclear peak is shown in (d) for comparison.

per Fe site and transition temperature decrease as the Sr concentration is increased [16]. This suggests that Fe^{3+}–O–Fe^{4+} as well as Fe^{4+}–O–Fe^{4+} exchange interactions are negligible up to this concentration. These observations lead us to conclude that Fe^{4+} remains disordered and only Fe^{3+} ions contribute to the antiferromagnetic interactions in $La_{0.7}Sr_{0.3}FeO_3$.

When we consider a hypothetical situation in which all the Fe^{3+} ions (70%) couple antiferromagnetically then we expect a moment of 3.22 μ_B on the Fe ion, taking 4.6 μ_B as the base value for the parent compound $LaFeO_3$. At the other extreme, considering 30% of Fe^{3+} to have Fe^{4+} as first-nearest neighbour and hence not contributing to the antiferromagnetic exchange interaction then the expected magnetic moment arising due to the remaining (i.e. 40%) Fe^{3+} ions will be 1.84 μ_B. In a random statistical distribution of Fe^{4+} ions in the matrix of Fe^{3+} ions the best available option is to take the average of the two extreme situations, which gives a value of 2.53 μ_B per Fe site, which is close to the observed value of 2.52 μ_B.

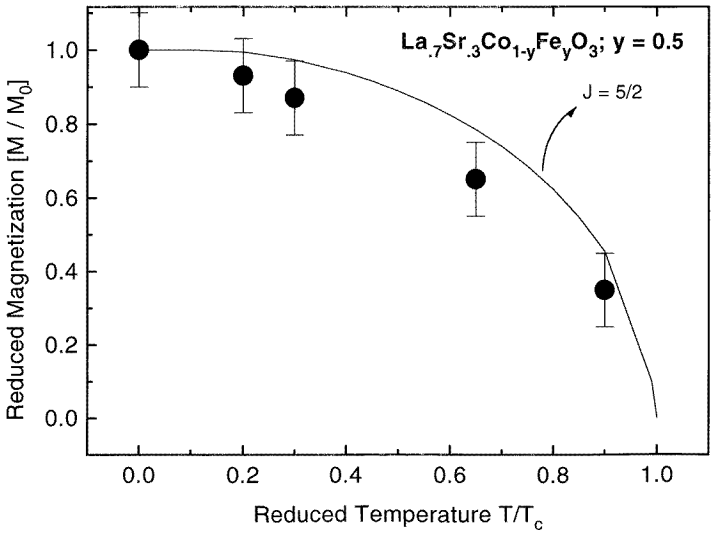

Figure 5. The temperature dependence of antiferromagnetic moment for $y = 0.5$ along with the Brillouin function for $S = 5/2$.

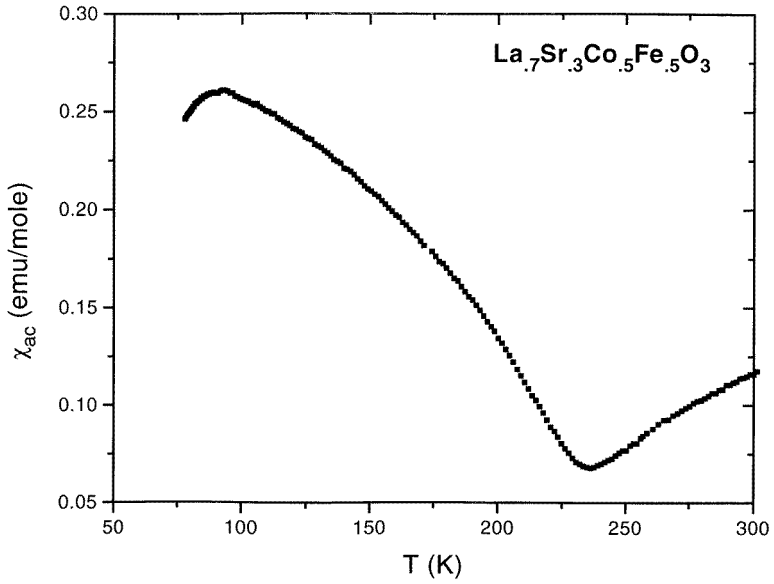

Figure 6. χ_{ac} against temperature from 80 K to 300 K for $y = 0.5$.

4.3. Intermediate compositions ($y = 0.5, 0.7$)

The $y = 0.7$ sample shows an antiferromagnetic order at room temperature. The magnetic moment calculated from the observed data is found to be 0.7 μ_B per TM ion at 297 K. The susceptibility measurements show two transition temperatures similar to the $y = 0.5$ composition.

The antiferromagnetic moment per TM ion in the $y = 0.5$ sample is 1.2 μ_B at 10 K which is almost half of the value observed for the $y = 1.0$ sample. As we have seen in the two end members ($y = 0.0, 1.0$) of this series the magnetic moment per TM ion is 1.89 μ_B and 2.52 μ_B. Proceeding on the same line of argument and a statistical random distribution of Co and Fe on this TM site the average expected antiferromagnetic moment is 0.63 μ_B which is much less than the observed moment (1.2 μ_B). This leads one to think in terms of a two-lattice model with Co-rich and Fe-rich regions. A similar argument has been used in the case of pure systems where observed magnetic moment is explained in terms of La- and Sr-rich regions [12].

For mixed composition as in the present compounds the situation is complex since both the ferro- and antiferromagnetic interactions are comparable. The contributing interactions may arise from (A) Fe^{3+}–O–Fe^{3+}, (B) Fe^{3+}–O–Fe^{4+}, (C) Co^{3+}–O–Co^{3+}, (D) Co^{3+}–O–Co^{4+}, (E) Co^{4+}–O–Fe^{3+}, (F) Co^{4+}–O–Fe^{4+}. Out of these configurations only (A) and (E) will result in negative exchange coupling giving antiferromagnetic order. All the other configurations will lead to double-exchange interaction giving rise to ferromagnetic order [12, 13, 25] except for configuration (C). For configuration (C) the positive exchange is established by polarized neutron diffraction studies in pure $LaCoO_3$ [10]. As the ferromagnetic correlations observed in Co^{3+}–O–Co^{3+} exchange are found to be many orders of magnitude smaller in $LaCoO_3$ than in $La_{1-x}Sr_xCoO_3$, we neglect this interaction in the present situation. Kawasaki *et al* [25] observed predominant ferromagnetic correlations in the $SrFe_{1-x}Co_xO_3$ system. The dominance of ferromagnetic correlations over antiferromagnetic correlations is explained by a simple picture in which Fe^{4+} ions with 4 μ_B and Co^{4+} ions with 1.8 μ_B align their moments ferromagnetically. Hence the possibility of (F) type interactions for ferromagnetic order cannot be completely ruled out. On the other hand the behaviour of the susceptibility with temperature for $y = 0.5$ (figure 6) and $y = 0.0$ [12] shows that in both the cases the ferromagnetic order starts to be set up around 230 K. This suggests that the interaction responsible for the ferromagnetic order in both the systems is the same, being a Co^{3+}–O–Co^{4+} double-exchange interaction.

5. Summary

Neutron diffraction measurements have been made to reveal the structural and magnetic behaviour of $La_{0.7}Sr_{0.3}Co_{1-y}Fe_yO_3$ ($0.0 \leqslant y \leqslant 1.0$). Characteristic features of these measurements are

(1) $La_{0.7}Sr_{0.3}Co_{1-y}Fe_yO_3$ shows a structural transition from rhombohedral to orthorhombic structure in the region $y \approx 0.5$.

(2) For Co-rich compounds ($y = 0.1, 0.2$) ferromagnetic order is observed.

(3) For the $y = 0.5$ sample both ferro- and antiferromagnetic order is seen.

(4) The $y = 1.0$ sample showed pure antiferromagnetic order with G-type structure and moment lying along the [100] direction.

Acknowledgments

VGS would like to thank Bhaba Atomic Research Centre for kind hospitality during the experimental work at the Dhruva reactor. We would also like to acknowledge Ms Ashna Bajpai and Dr Alok Banerji for susceptibility measurements.

References

[1] Jonker G H and Van Santen J H 1950 *Physica* **16** 337
Jonker G H and Van Santen J H 1950 *Physica* **16** 559
[2] Reccah P M and Goodenough J B 1967 *Phys. Rev.* **155** 932
[3] Jin S, Tiefel T H, McCormack M, Fastnacht R A, Ramesh R and Chen L H 1994 *Science* **264** 413
[4] McCormack, Jin S, Tiefel T H, Fleming R M, Phillips J M and Ramesh R 1994 *J. Appl. Phys. Lett.* **64** 3045
[5] Von Helmholt R, Wecker J, Holzapfel B, Schultz L and Samwer K 1993 *Phys. Rev. Lett.* **71** 2331
[6] Asamitsu A, Moritomo Y, Tomioka Y, Arima J and Tokura Y 1995 *Nature* **373** 405
[7] *Landolt–Börnstein New Series* 1970 Group III, vol 4a (Berlin: Springer)
[8] Hwang H Y, Cheong S W, Radaelli P G, Marezio M and Batlogg B 1995 *Phys. Rev. Lett.* **75** 914
[9] Bhide V G, Rajoria D S, Rao G R and Rao C N R 1972 *Phys. Rev.* B **6** 1021
[10] Asai K, Yokokura O, Nishimori, Chou H, Tranquada J M, Shirane G, Higuchi S, Kijma Y O and Kohn K 1994 *Phys. Rev.* B **50** 3025
[11] Bhide V G, Rajoria D S, Rao C N R and Jadhao V G 1975 *Phys. Rev.* B **12** 2832
[12] Sathe V G, Pimpale A V, Siriguri V and Paranjpe S K 1996 *J. Phys.: Condens. Matter* **8** 3889
[13] Zener C 1951 *Phys. Rev.* **81** 440
Zener C 1951 *Phys. Rev.* **82** 403
[14] De Gennes P G 1960 *Phys. Rev.* B **118** 141
[15] Itoh M, Natori I, Kubota S and Motoya K 1994 *J. Phys. Soc. Japan* **63** 1468
[16] Grenier J C, Ea N, Pcchard M and Abou-Sekkina M M 1984 *Mater. Res. Bull.* **19** 1301
[17] Li J Q, Matsui Y, Park S K and Tokura Y 1997 *Phys. Rev. Lett.* **79** 297
[18] Paranjpe S K and Dande Y D 1989 *Pramana* **32** 793
[19] Young R A, Sakthivel A, Moss T S and Paivasantos C O 1994 *User's Guide to Program DBWS-9411* (GA: Georgia Institute of Technology)
[20] Rodriguez-Carvajal J 1995 *FULLPROF* version 3.0.0, Laboratoire Leon Brillouin, CEA–CNRS
[21] Koehler W C, Wollan E O and Wilkinson M K 1960 *Phys. Rev.* **118** 58
[22] Senaris M A and Goodenough J B 1995 *J. Solid State Chem.* **118** 323
[23] Minet Y, Lefranc V, Nguyen N, Domenges B, Maignan A and Reveau B 1996 *J. Solid State Chem.* **121** 158
[24] Koehler W C and Wollan E O 1957 *J. Phys. Chem. Solids* **2** 100
[25] Kawasaki S, Takano M and Takeda Y 1996 *J. Solid State Chem.* **121** 174